

1 Detecting Solution pH Changes Using Poly (*N*-
2 Isopropylacrylamide)-*co*-Acrylic Acid Microgel-
3 Based Etalon Modified Quartz Crystal
4 Microbalances

5 Kai C.C. Johnson, Francisco Mendez, and Michael J. Serpe*

6 Department of Chemistry, University of Alberta, Edmonton, AB, T6G 2G2

7 * To whom correspondence should be addressed: michael.serpe@ualberta.ca

8 **Abstract:** Poly (*N*-isopropylacrylamide)-*co*-acrylic acid (pNIPAm-*co*-AAc) microgel-based
9 etalons have been shown to have visible color and unique spectral properties, which both depend
10 on solution temperature and pH. In this investigation, pNIPAm-*co*-AAc microgel-based etalons
11 were fabricated on the Au electrode of a quartz crystal microbalance (QCM), and the resonant
12 frequency of the QCM monitored as a function of temperature, at pH 3.0. Furthermore, the
13 resonant frequency at either pH 3.0 or 7.0 was monitored while keeping the solution temperature
14 constant at various temperatures. In all cases, when the solution temperature was below the
15 collapse transition for the microgels (~32 °C), the resonant frequency at pH 3.0 was lower than at
16 pH 7.0, which we attribute to the film transitioning from a deswollen to swollen state ,
17 respectively. It was observed that the magnitude of the resonant frequency change increased as
18 the solution temperature approached the collapse temperature for the microgels. The overall
19 sensitivity to pH was determined to be $1.3 \times 10^{-8} \text{ M } [\text{H}^+] \text{ Hz}^{-1}$ and a theoretical detection limit of

20 390 nM was obtained. This sensitivity will be exploited further for future biosensing
21 applications.

22 **Keywords:** Poly (N-isopropylacrylamide) microgels, color tunable materials, quartz crystal
23 microbalance, stimuli responsive polymers, sensing

24

25 **1. Introduction**

26 Poly (*N*-isopropylacrylamide) (pNIPAm) is one of the most well-known and extensively
27 studied thermoresponsive polymers. At $T < 32\text{ }^{\circ}\text{C}$, pNIPAm is fully water soluble, existing as a
28 random coil. At $T > 32\text{ }^{\circ}\text{C}$, pNIPAm transitions from a hydrated random coil to a desolvated,
29 compact globule.[1-3] The temperature at which this occurs is called the lower critical solution
30 temperature (LCST), or the volume phase transition temperature.[4] The thermoresponsive
31 nature of linear pNIPAm can be used to synthesize pNIPAm-based particles (microgels) via free
32 radical precipitation polymerization.[5-11] Microgels are extremely porous, and like their linear
33 polymer counterparts, are fully water soluble (and water swollen, large diameter) at $T < \text{LCST}$,
34 and expel their solvating water and collapse (small diameter) at $T > \text{LCST}$. When microgels
35 expel their solvating water their viscosity increases.[12] PNIPAm microgels are also quite easily
36 modified with other functional groups, typically via copolymerization of comonomers into the
37 microgel at the time of synthesis. The most commonly used comonomer is acrylic acid (AAc).
38 AAc is a weak acid, which has a pK_a of ~ 4.25 , therefore, at $\text{pH} < \text{pK}_a$ the pNIPAm based
39 microgels are fully responsive, while at $\text{pH} > \text{pK}_a$ the pNIPAm responsivity is hindered.[13-16]
40 That is, at $\text{pH} > \text{pK}_a$ the Coulombic repulsion between the deprotonated AAc groups in the
41 microgels prevents their collapse at $T > 32\text{ }^{\circ}\text{C}$, requiring significantly higher T to achieve a
42 microgel response. AAc not only results in pH responsive pNIPAm microgels, but the AAc

43 groups can also be used as reactive “handles” to add further functionality to the microgels.[17,
44 18]

45 We have recently demonstrated that pNIPAm-*co*-AAc microgels can be used to fabricate
46 color tunable materials by “painting” a very uniform microgel layer onto metal coated
47 supports.[19-24] The resulting microgel layer can subsequently be coated with another thin
48 metal layer to yield a microgel layer “sandwiched” between two semi-transparent (yet
49 reflective) metal layers. Figure 1 shows a schematic for the assembly. We have shown that when
50 these devices (etalons) are immersed in water, they exhibit visible color due to light interference
51 in the cavity formed between the two Au layers. The specific color depends on the distance
52 between the mirrors. Since the microgel’s diameter depends on temperature, the distance
53 between the mirrors can be changed, and hence the etalon’s color dynamically tuned.[19-25] In
54 this submission we exploit the solvation state changes that take place when an etalon changes
55 color, as opposed to exploiting the actual color change, for sensing purposes. This is done by
56 immobilizing the etalon on the Au electrode of an AT-cut quartz crystal microbalance (QCM).

57 An AT-cut QCM crystal can be excited electrically to undergo an oscillating shearing
58 motion, at a characteristic resonant frequency (most commonly 5 MHz). The resonant frequency
59 is dependent on the properties (e.g., mass, viscosity) of the material in contact with the
60 oscillating device and is described by equation (1): [26]

61

$$62 \quad \Delta f = -f_0^{\frac{3}{2}}(n_l p_l / \pi p_q \mu_q)^{1/2} \quad (1)$$

63

64 Where f_0 is the initial resonant frequency of the QCM crystal, Δf is the frequency shift measured
65 by the quartz crystal microbalance, ρ_l is the liquid density, η_l is the liquid viscosity, μ_q is the
66 elastic modulus of quartz, and ρ_q is the density of quartz.[26]

67 As shown by Kanazawa and others,[27,28] and is apparent in equation (1), the resonant
68 frequency of the QCM decreases as the viscosity of the substance contacting the QCM crystal
69 increases. Furthermore, increased viscosity leads to an increase in the “resistance” of QCM
70 oscillation.

71 Here, we demonstrate that pNIPAm microgel-based etalons can be fabricated on the Au
72 electrode of a quartz crystal microbalance (QCM). While the etalons still function as an optical
73 device, see Figure 2 for a sample reflectance spectrum, we show that the resonant frequency of
74 the QCM crystal likewise depends on solution T and pH. We hypothesize that the frequency
75 shifts in response to viscosity changes that occur when the microgels transition from a swollen
76 (low viscosity) to a deswollen (high viscosity) state.[12] As we show here, this phenomenon can
77 be exploited for pH sensing, although this phenomenon can be exploited to detect other species
78 that interact with the microgels of the etalons that result in a microgel solvation change.

79 **2. Experimental**

80 *2.1. Materials*

81 *N*-Isopropylacrylamide was purchased from TCI (Portland, Oregon) and purified by
82 recrystallization from hexanes (ACS reagent grade, EMD, Gibbstown, NJ) prior to use. *N,N'*-
83 methylenebisacrylamide (BIS) (99%), acrylic acid (AAc) (99%), and ammonium persulfate
84 (APS) (98+%) were obtained from Sigma-Aldrich (Oakville, ON) and were used as received.
85 Sodium chloride and sodium hydroxide were obtained from Fisher (Ottawa, ON). All deionized
86 (DI) water was filtered to have a resistivity of 18.2 M Ω · cm and was obtained from a Milli-Q

87 Plus system from Millipore (Billerica, MA). Cr and Au were deposited using a Model THEUPG
88 Thermal Evaporation System from Torr International Inc. (New Windsor, NY). Anhydrous
89 ethanol was obtained from Commercial Alcohols (Brampton, ON). Hydrochloric acid was
90 purchased from Caledon Chemicals (Georgetown, ON). Cr was 99.999% and obtained from
91 ESPI (Ashland, OR), while Au was 99.99% obtained from MRCS Canada (Edmonton, AB).

92 *2.2. Instrumentation*

93 Microgel coated QCM crystals, as well as the etalon coated devices were analyzed using a QCM-
94 200 obtained from Stanford Research Systems (Sunnyvale, CA). The crystal was placed into a
95 specially designed holder, which allowed for water of a given pH and temperature to constantly
96 flow over the crystal at a rate of 0.062 mL/s. This flow was maintained by a FMI lab pump
97 model RP-G150 (Oyster Bay, NY). The temperature was controlled by placing a beaker
98 containing water onto a Corning model PC-420D hotplate (Lowell, MA), and the water
99 temperature measured via a thermocouple. To change the pH of the solution, aliquots of either
100 1M NaOH or concentrated HCl were added to the water, and the water pH measured with a
101 Jenco model 6173 pH meter (San Diego, CA). Ionic strength was not controlled, but we
102 confirmed that changes in ionic strength had little effect on the resonant frequency of the QCM
103 crystal (data not shown).

104 *2.3. Procedures*

105 *2.3.1. Microgel synthesis*

106 The microgels used in this study were synthesized using surfactant-free, free radical
107 precipitation procedure as described previously.[12, 19-25] Briefly, 8.5 mmol of NIPAM and
108 0.51 mmol of N,N'-methylenebisacrylamide (BIS) was added to a beaker, and dissolved in 50

109 mL of deionized water. Once dissolved, the solution was filtered via a syringe through a 0.2 μm
110 syringe filter into a 100 mL 3-necked round bottom flask containing a stir bar. 12.5 mL of
111 deionized water was used to rinse the beaker, which was also filtered and added to the round
112 bottom flask. Next, a gas inlet (needle), a reflux condenser, and a temperature probe were fitted
113 onto the round bottom flask. The solution was stirred at 450 RPM, and purged free of O_2 by
114 bubbling N_2 gas through the solution while heating to 45 $^\circ\text{C}$ for 1 h. Immediately prior to
115 initiation, 1 mmol of AAc was added to the solution along with 2.5 mL of 0.078 M ammonium
116 persulfate solution. The solution temperature was then increased to 65 $^\circ\text{C}$ at a rate of 30 $^\circ\text{C}/\text{hour}$
117 immediately following initiation and was allowed to react overnight. Following the overnight
118 reaction, the solution was allowed to cool and was filtered through glass wool to remove large
119 aggregates from the solution. The filtrate was then diluted to 120 mL with deionized water and
120 12 mL aliquots were added to centrifuge tubes, and centrifuged at ~ 8500 relative centrifugal
121 force for 30 minutes each at 20 $^\circ\text{C}$. The microgels were packed at the bottom of the centrifuge
122 tube, and the supernatant solution subsequently removed, and replaced with fresh DI water.
123 Centrifugation and resuspension was repeated five more times to remove any unreacted reagents
124 present.

125 *2.3.2. Formation of etalons on QCM crystals*

126 Etalons were fabricated as previously described, with some slight modification.[19-24]
127 The Au electrodes of the QCM quartz crystal were rinsed copiously with anhydrous ethanol and
128 dried with N_2 gas. 12.5 μL of a concentrated, viscous microgel solution was “painted” only on
129 the “large” Au electrode of the QCM crystal and allowed to dry for 30 minutes at 35 $^\circ\text{C}$.
130 Following drying, the microgels not directly bound to the Au electrode were rinsed off with DI
131 water, and the QCM crystal was immersed in DI water overnight at 35 $^\circ\text{C}$. Following soaking, the

132 crystal was further rinsed with DI water and dried with N₂ gas. A paper template was adhered to
133 the QCM crystal, such that only the Au electrode, which was coated with microgels was
134 exposed. The QCM crystal was then inserted into a Torr International Inc.(New Windsor, NY)
135 thermal evaporation system Model THEUPG. 2 nm of Cr and 15 nm of Au were deposited only
136 onto the Au bound microgel layer at a rate of $\sim 0.2 \text{ \AA s}^{-1}$ and $\sim 0.1 \text{ \AA s}^{-1}$, for Cr and Au,
137 respectively. After application of this overlayer, the crystal was subsequently removed from the
138 vacuum chamber and immersed in DI water overnight at 35°C. The QCM bound etalon was
139 subsequently used.

140

141 **3. Results and discussion**

142 *3.1. Temperature responsivity*

143 PNIPAm-*co*-AAc microgels with an average diameter of $1.5 \pm 0.2 \text{ \mu m}$ (measured via
144 optical microscopy) were painted on the Au electrode of a QCM crystal. A differential
145 interference contrast microscope image of the microgels is shown in Figure 3. The behavior of
146 the QCM bound microgels was investigated by monitoring the resonant frequency of the QCM
147 crystal, as the temperature of the pH 3.0 solution was raised, which affects the solvation state of
148 the microgels. As can be seen in Figure 4(a), the crystal's resonant frequency decreased as the
149 temperature of the pH 3.0 solution was ramped from 22.6 °C to 35.8 °C at an average rate of
150 0.001 °C/s. The frequency reached a minimum close to 32 °C, which is the accepted LCST for
151 pNIPAm-*co*-AAc microgels at pH 3.0. The total observed frequency change from the initial
152 temperature to the transition temperature was 4260 Hz. The QCM frequency surprisingly
153 increased as the solution temperature exceeded the collapse temperature. We hypothesize that the
154 observed frequency shift with increasing temperature, up to the microgel's LCST, is a result of

155 the increased viscosity of the collapsed microgels.[12] Figure 4(b) shows the behavior of the
156 same microgels after deposition of a 2 nm Cr/15 nm Au layer on top of the microgels. Similar to
157 the uncoated microgels, the etalon caused the QCM crystal frequency to decrease as the
158 temperature of the pH 3.0 solution was increased from 24.2 °C to 35.3 °C at an average rate of
159 0.001 °C/s. As can be seen from the data, the 6903 Hz frequency change of the etalon is much
160 more dramatic than what was observed for the uncoated microgels. At this point, the reason for
161 the enhanced response of the etalon coated QCM crystal to temperature is unknown. Although, it
162 is known that at high temperature the Au layer on top of the microgels will be close to the QCM
163 crystal surface, as a result of the microgels collapsing.[19-25] As a result, the QCM crystal will
164 be able to detect the increased viscosity from the collapsed microgels as well as the mass of the Au
165 overlayer. This combined will lead to a greater QCM response. To confirm that this observed
166 behavior was due to the microgels, and not the crystal's sensitivity to temperature, an uncoated
167 QCM crystal was heated, in the same way as above, which shows a relatively small frequency
168 response to temperature. Therefore we attribute the frequency changes to the presence of the
169 microgels and etalon on the QCM crystal's Au electrode.

170 We wanted to further confirm that the observed behavior was truly due to the microgels,
171 and the microgel's influence on the QCM crystal, and not due to heating the microgels at non-
172 equilibrium conditions, i.e., a continuous temperature ramp as was done above. To do this, the
173 samples used to generate the data in Figures 4(a) and 4(b) were heated to discrete temperatures,
174 and the frequency allowed to stabilize. Figures 5(a) and 5(b) show the frequency data as a
175 function of time, at various temperatures, for the uncoated and Cr/Au coated microgels (etalons).
176 As can be seen, the trends for the QCM resonant frequency were similar to the continuous
177 heating experiments. Most important for the study here is the ability to stabilize the QCM's

178 frequency at each temperature, especially at the minimum found at the LCST. Figure 6 shows the
179 resonant frequency values at each stabilization temperature for the uncoated microgels and the
180 etalon. As can be seen from the data, if the microgel layer can be made to reswell, while
181 maintaining the solution temperature at the LCST, a large QCM frequency shift, back toward its
182 frequency at low temperature would be expected.

183 *3.2. pH responsivity*

184 To investigate this further, we took advantage of the pH responsivity of the pNIPAm-co-
185 AAc microgels. It is well known that at a given temperature, the diameter of pNIPAm-co-AAc
186 microgels is larger at pH 7.0 than at pH 3.0. In other words, the viscosity of the microgels at pH
187 7.0 will be lower than at pH 3.0. Therefore, it stands to reason that at all temperatures, the QCM
188 resonant frequency at pH 7.0 should be higher than at pH 3.0. Figures 7(a) and 7(b) show that for
189 both the uncoated microgel layer, and the etalons, that this is the case. From the plots, it appears
190 that a pH change from 3.0 to 7.0 is enough to reswell the collapsed microgels, and affords a
191 frequency increase. In fact, because the change in the QCM crystal frequency, relative to its
192 initial value, is much greater compared to the uncoated microgels, the frequency change upon
193 reswelling at high pH is likewise enhanced. In addition, in both cases it can be seen that the
194 QCM frequency at the LCST in pH 7.0 solution was greater than its frequency at low
195 temperature in pH 3.0 solution. We hypothesize that this is a result of Coulombic repulsion
196 between the deprotonated AAc groups in the microgels at pH 7.0 causing the microgels to be
197 more swollen (less viscous) than they are at low temperature in pH 3.0 solution. This is a well-
198 known phenomenon for pNIPAm-co-AAc microgels in solution. [12] The resulting changes in
199 frequency in response to the solution pH change for the uncoated microgel layer and after Cr/Au
200 addition were 5401 Hz and 8217 Hz, respectively.

201 We further investigated whether the pH response could be enhanced at any other
202 temperature. To accomplish this, pH transitions from 3.0 to 7.0 were performed at multiple
203 temperatures. As seen in Figures 8(a) and 8(b), the QCM crystal frequency plateaus at similar
204 values after transitioning from pH 3.0 to 7.0. This means that the film's reswelling is limited;
205 therefore the maximum pH response is achieved when the film is at the LCST. In other words,
206 the maximum response is achieved when the microgels transition from their fully collapsed to
207 fully swollen form. The fact that the QCM crystal's frequency returns to the same maximum
208 resonant frequency in pH 7.0 solution at each temperature further supports the hypothesis that
209 the microgels reswell in pH 7.0 solution due to Coulombic repulsion.

210 Finally, we set out to find the pH range that the device would be most sensitive. To
211 determine this, the etalon was brought to its transition temperature at pH 3.0. At this temperature,
212 the solution's pH was increased stepwise, while monitoring the QCM resonant frequency. The
213 resonant frequency was allowed to stabilize at each pH value investigated, and the solution pH
214 was continuously monitored. Figures 9(a) and 9(b) show the results of this experiment for both
215 an uncoated microgel layer and an Au coated microgel layer. Each pH value stated was stabilized
216 for at least 15 minutes before further addition of NaOH. As can be seen, the maximum response
217 occurs over a two (2) pH unit range, centered around a pH of ~4.10, which is close to the
218 accepted value for the pK_a for AAc. From the data, we estimated the device's detection limit to
219 be 390 nM H^+ , with a sensitivity was calculated to be $1.3 \times 10^{-8} [H^+] \text{ Hz}^{-1}$. From the data, it also
220 stands to reason that in order to make an etalon that is sensitive in other pH ranges, acidic
221 monomers with varying pK_a 's can be polymerized into the microgels.

222 4. Conclusions

223 In this submission, we showed that the resonant frequency of a microgel coated QCM
224 crystal (and etalon) was affected dramatically by the temperature and pH of the solution it was
225 exposed to. We hypothesize that this response was a result of the different solvation states (and
226 hence viscosity) of the microgels as a function of temperature and pH. This sensitivity was
227 exploited for pH sensing, by operating the materials at the microgels LCST. The response to pH
228 was shown to be more significant for the Cr/Au coated microgel layers (etalons). The most
229 sensitive region for the samples is at the LCST over 1 pH unit range. We can detect pH shifts as
230 little as 390 nM [H+] within this pH range. This system will be further developed for biosensing
231 applications as well as for detecting pH changes in different ranges.

232 **Acknowledgements:** MJS acknowledges funding from the University of Alberta (the
233 Department of Chemistry and the Faculty of Science), the Natural Science and Engineering
234 Research Council (NSERC), the Canada Foundation for Innovation (CFI), and the Alberta
235 Advanced Education & Technology Small Equipment Grants Program (AET/SEGP). MJS
236 acknowledges Mark McDermott for the use of the thermal evaporator. MJS would also like to
237 thank Prof. L. Andrew Lyon for intellectual contributions to this project.

238 **References:**

- 239 [1] Wu, C. Wang, X. Phys. Rev. Lett. 80 (1998) 4092–4094.
240 [2] Zhang, G. Wu, C. Phys. Rev. Lett. 85(5) (2001) 822-825.
241 [3] Xu, J. Zhu, Z. Luo, S. Wu, C. Liu, S. Phys. Rev. Lett. 96(2) (2006) 027802.
242 [4] Wu, C. Zhou, S. Macromolecules. 28 (1995) 8381-8387.
243 [5] Jones, C.D. Lyon, L.A. Macromolecules. 33 (2000) 8301–8306.
244 [6] Horgan, A. Saunders, B. Vincent, B. Heenan, R.K. J. Colloid Interface Sci. 262(2)
245 (2003) 548-559.

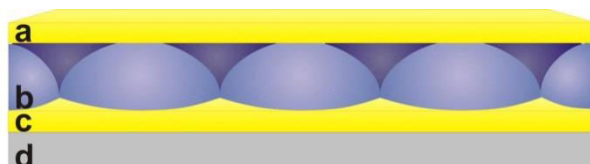
- 246 [7] Liu, J. Pelton, R. Hrymak, A.N. J. Colloid Interface Sci. 227(2) (2000) 408-411.
- 247 [8] Karg, M. Pastoriza-Santos, I. Rodriguez-Gonzalez, B. von Klitzing, R. Wellert, S.
248 Hellweg, T. Langmuir. 24(12) (2008) 6300-6306.
- 249 [9] Tsuji, S. Kawaguchi, H. Langmuir. 20(6) (2004) 2449-2455.
- 250 [10] Dean G.R. Alsted, T. Richtering, W. Pedersen, J.S. Phys. Chem. Chem. Phys.
251 13(8) (2011) 3108-3114.
- 252 [11] Crassous, J.J. Ballauff, M. Drechsler, M. Schmidt, J. Talmon, Y. Langmuir. 22(6)
253 (2006) 2403-2406.
- 254 [12] Serpe, M.J. Lyon, L.A. Chem. Mater. 16 (2004) 4373-4380.
- 255 [13] Smith, M.H. Lyon, L.A. Macromolecules. 44(20) (2011) 8154-8160.
- 256 [14] Hu, X. Tong, Z. Lyon, L.A. J. Am. Chem. Soc. 132(33) (2010) 11470-11472.
- 257 [15] Pei, Y. Chen, J. Yang, L. Shi, L. Tao, Q. Hui, B. Li, J. J. Biomater. Sci. Polym.
258 Ed. 15(5) (2004) 585-594.
- 259 [16] Wei, J.S. Zeng, H.B. Liu, S.Q. Wang, X.G. Tay, E.H. Yang, Y.Y. Front. Biosci.
260 10 (2005) 3058-3067.
- 261 [17] Debord, J. Lyon, L.A. Bioconjugate Chem. 18(2) (2007) 601-604.
- 262 [18] Huang, W.C. Chiang, W.H. Huang, Y.F. Lin, S.C. Shih, Z.F. Chern, C.S. Chiang,
263 C.S. Chiu, H.C. J. Drug Targeting. 19(10) (2011) 944-953.
- 264 [19] Sorrell, C.D. Carter, M.C.D Serpe, M.J ACS Appl. Mater. Interfaces. 3(4) (2011)
265 1140–1147.
- 266 [20] Carter, M.C.D. Sorrell, C.D. Serpe, M.J. J. Phys. Chem. B. 115(49) (2011) 14359-
267 14368.
- 268 [21] Hu, L. Serpe, M.J. J. Mater. Chem. 22 (2012) 8199-8202.

- 269 [22] Hu, L. Serpe, M.J. *Polymers*. 4(1) (2012) 134-149.
- 270 [23] Sorrell, C.D. Serpe, M.J. *Anal. Bioanal. Chem.* 402 (2012) 2385-2393.
- 271 [24] Sorrell, C.D. Serpe, M.J. *Adv. Mater.* 23(35) (2011) 4088-4092.
- 272 [25] Sorrell, C.D. Carter, M.C.D. Serpe, M.J. *Adv. Funct. Mater.* 21 (2011) 425-433.
- 273 [26] Kanazawa, K.K. Gordon, J.G. *Anal. Chim. Acta.* 175 (1985) 99-105.
- 274 [27] Lee, S.W. Hinsberg, W.D. Kanazawa, K.K. *Anal. Chem.* 74(1) (2002) 125-31.
- 275 [28] Ward, M.D. Buttry, D.A. *Science*. 249(4972) (1990) 1000-1007.
- 276 [29] Lyon, L.A. Meng, Z. Singh, N. Sorrell, C.D. St. John, A. *Chem. Soc. Rev.* 38
277 (2009) 865-874.

278

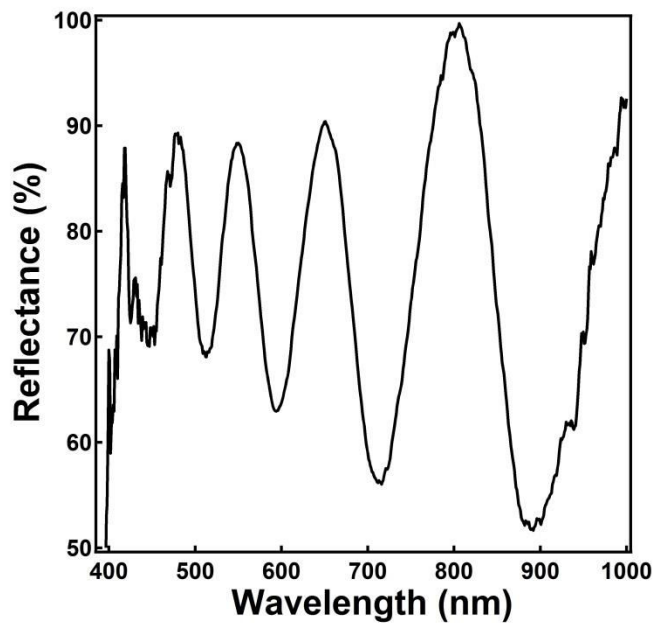
279

280 **Figures:**



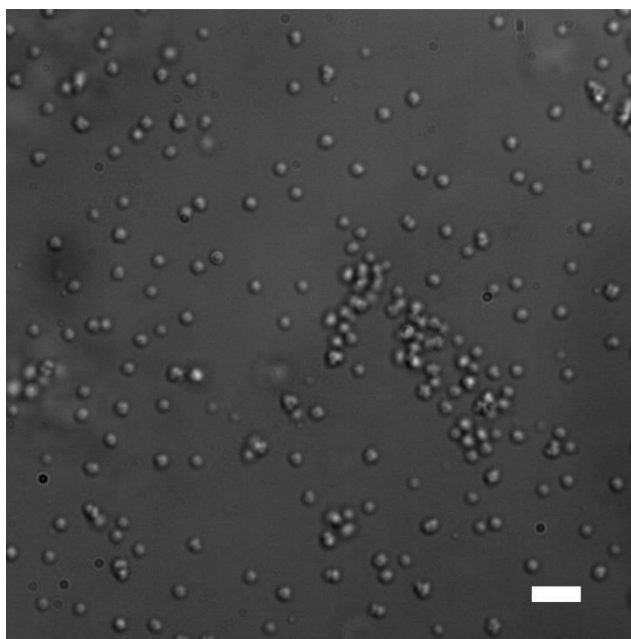
281

282 **Figure 1.** Structure of a poly (N-isopropylacrylamide) microgel-based etalon. (a and c) two 15
283 nm Au mirrors (with 2 nm Cr adhesion layer) sandwiching (b) the microgel layer. Typically, (d)
284 is a glass substrate. For these experiments, (d) is an AT-cut quartz crystal.



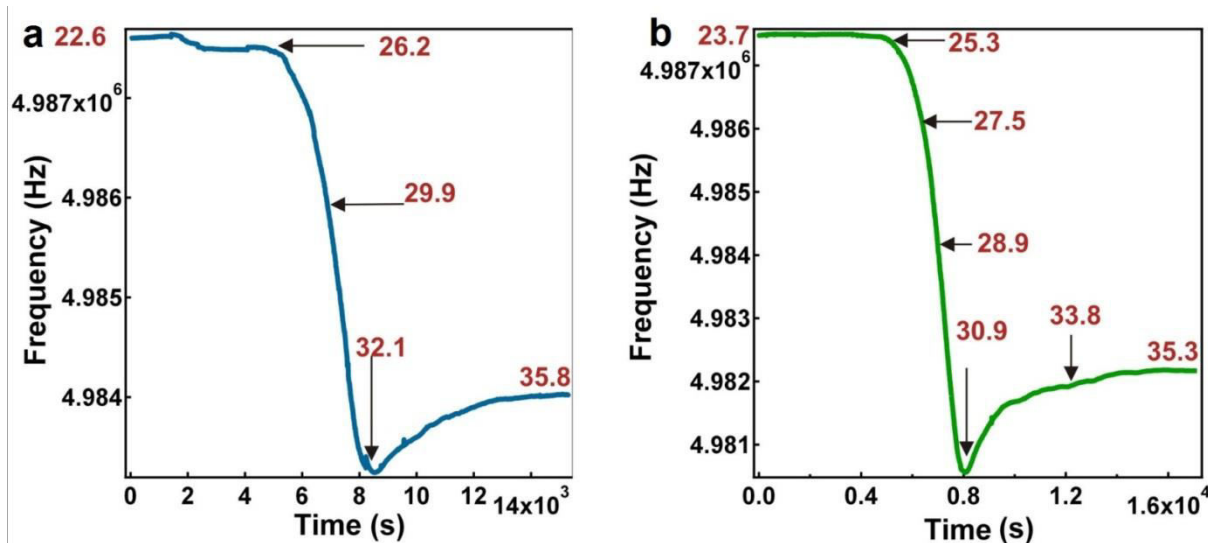
285

286 **Figure 2.** Reflectance spectrum of a representative etalon immobilized on a QCM crystal. The
287 various peaks correspond to the different orders of reflection, which is typical of pNIPAm
288 microgel-based etalons.

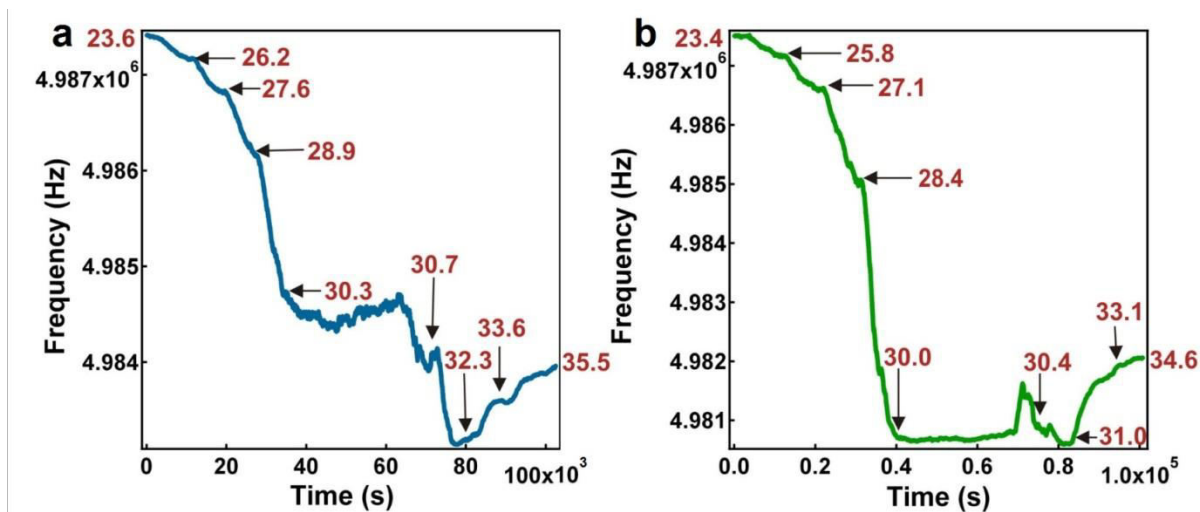


289

290 **Figure 3.** Differential interference contrast microscope image of the pNIPAm-based microgels
291 used in this study. The microgels were in water, on a glass substrate. The scale bar is 6 μm .



292
293 **Figure 4.** QCM resonant frequency as a function of time for (a) pNIPAm-*co*-AAc microgel
294 coated QCM crystal and (b) after deposition of a 2 nm Cr/15 nm Au overlayer in pH 3.0 water.
295 The heating rate was on average 0.001 $^{\circ}\text{C}/\text{s}$, and the values on the individual plots correspond to
296 the temperature ($^{\circ}\text{C}$) at a given time.

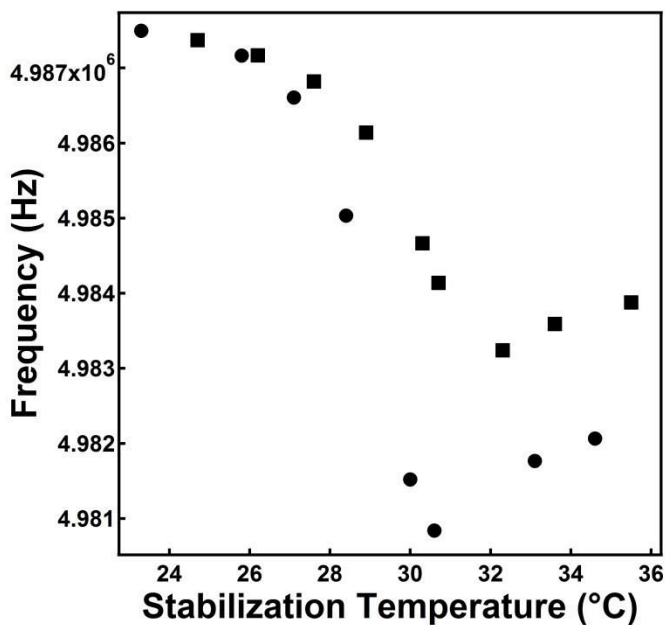


297
15

298 **Figure 5.** QCM resonant frequency as a function of time for (a) pNIPAm-*co*-AAc microgel
299 coated QCM crystal and (b) after deposition of a 2 nm Cr/15 nm Au overlayer in pH 3.0 water.
300 After reaching a given temperature, the QCM resonant frequency was allowed to stabilize before
301 proceeding to the next temperature. The values on the individual plots indicate the temperature
302 (°C) at the individual stabilization points.

303

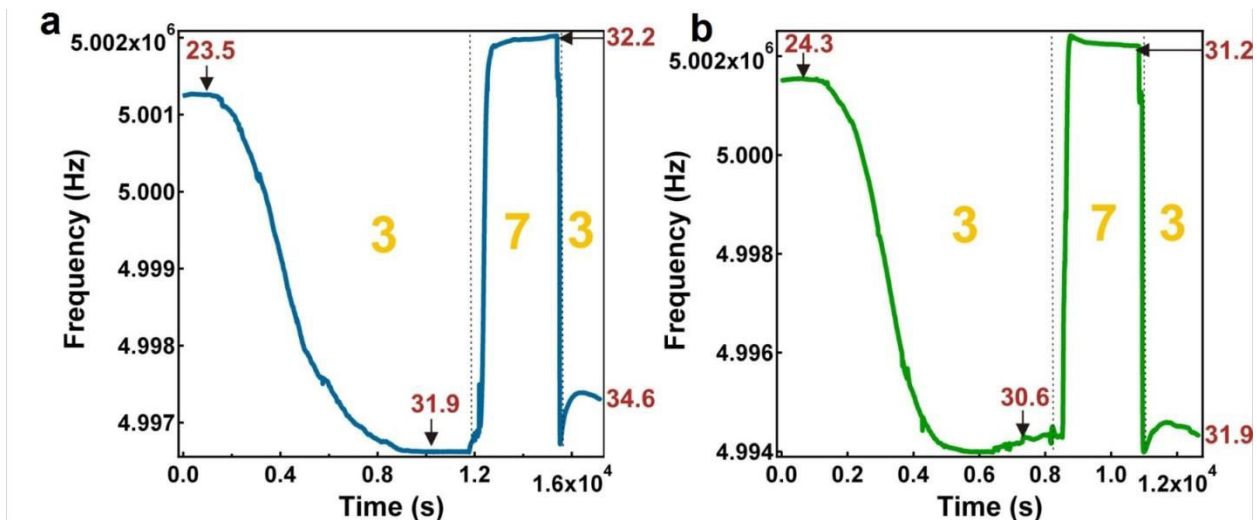
304



305

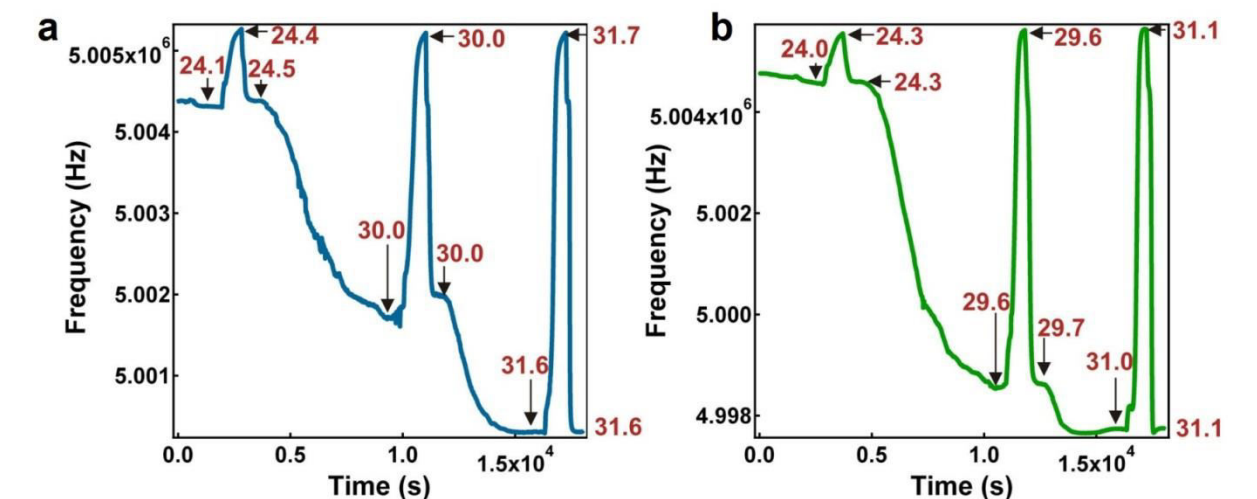
306 **Figure 6.** QCM resonant frequency at the individual stabilization temperatures in Figure 4. (■)
307 pNIPAm-*co*-AAc microgel coated QCM crystal and (●) after deposition of a 2 nm Cr/15 nm Au
308 overlayer in pH 3.0 water.

309



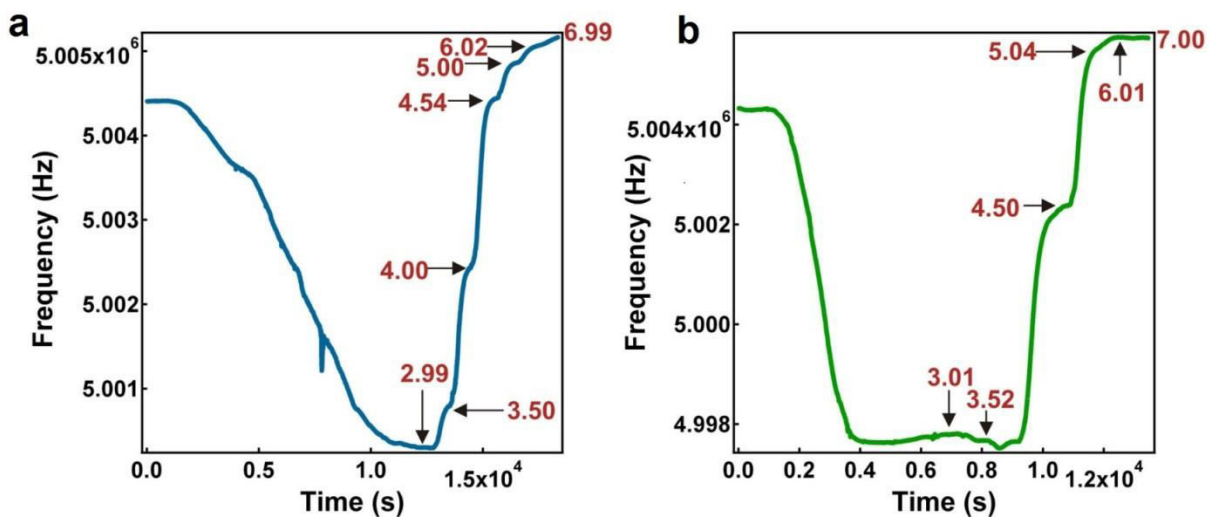
310 **Figure 7.** The pH response of a (a) pNIPAm-*co*-AAc microgel coated QCM crystal and (b) the
311 same substrate after deposition of a 2 nm Cr/15 nm Au overlayer. Initially, each was heated to
312 the film's lower critical solution temperature in pH 3.0 water. Following stabilization, the pH of
313 the water was increased to 7.0 by addition of 1M NaOH. Again, the signal was allowed to
314 stabilize, and the pH returned to 3.0 by addition of concentrated HCl. The pH and temperature
315 (°C) values are indicated on the individual plots.

316



317 **Figure 8.** The pH response of a (a) pNIPAm-*co*-AAc microgel coated QCM crystal and (b) the
318 same substrate after deposition of a 2 nm Cr/15 nm Au overlayer at different temperatures. In

319 each case, the QCM resonant frequency was allowed to stabilize at $\sim 24\text{ }^{\circ}\text{C}$ in pH 3.0 water.
 320 While maintain a similar temperature, the pH of the water was adjusted to 7.0 by addition of 1 M
 321 NaOH. The addition of NaOH is observed as an increase in QCM resonant frequency. Following
 322 QCM resonant frequency stabilization, the pH was again adjusted to 3.0 by addition of
 323 concentrated HCl. Following this step, in each case the temperature was adjusted to $\sim 30\text{ }^{\circ}\text{C}$ and
 324 $\sim 31\text{ }^{\circ}\text{C}$, and the pH modulation repeated at each temperature range.



325
 326 **Figure 9.** The pH response of a (a) pNIPAm-co-AAc microgel coated QCM crystal and (b) the
 327 same substrate after deposition of a 2 nm Cr/15 nm Au overlayer at the film's lower critical
 328 solution temperature. In each case, the films were exposed to pH 3.0 water and the temperature
 329 of the solution adjusted to the film's lower critical solution temperature of $\sim 31\text{-}32\text{ }^{\circ}\text{C}$. Following
 330 stabilization of the QCM resonant frequency, the pH of the solution was adjusted stepwise by
 331 addition of 1 M NaOH. The actual pH values are indicated on each plot.

332